

Petrogenetic Characterization of the Geological Formations of the Localities of Goumère-Iguela in the South West of the Bui Belt (North-East of Côte d'Ivoire)

Fossou Jean-Luc Hervé Kouadio*, Tokpa Kakeu Lionel-Dimitri Boya, N'Guessan Nestor Houssou, Roger Nicaise Kanga, Alain Nicasie Kouamelan

Laboratoire de Géologie, Ressources Minérales et Energétiques, Université Félix Houphouët-Boigny, Abidjan-Cocody, Côte d'Ivoire

Email: *fossoujean@gmail.com

How to cite this paper: Kouadio, F.J.-L.H., Boya, T.K.L.-D., Houssou, N.N., Kanga, R.N. and Kouamelan, A.N. (2022) Petrogenetic Characterization of the Geological Formations of the Localities of Goumère-Iguela in the South West of the Bui Belt (North-East of Côte d'Ivoire). *Open Journal of Geology*, 12, 947-972.

<https://doi.org/10.4236/oig.2022.1211045>

Received: September 16, 2022

Accepted: November 13, 2022

Published: November 16, 2022

Copyright © 2022 by author(s) and Scientific Research Publishing Inc. This work is licensed under the Creative Commons Attribution International License (CC BY 4.0).

<http://creativecommons.org/licenses/by/4.0/>



Open Access

Abstract

Located in the north-east of Côte d'Ivoire, the Gouméré-Iguéla sectors were the subject of a geological mapping. These geological formations are located southwest of the Bui trench. In order to improve the petrogenetic knowledge of the study area, a multidisciplinary methodology integrating microscopic observations and geochemical analyses of major and trace elements was carried out on 15 samples considered as representative of the studied outcrops. The macroscopic and microscopic petrographic study allowed to highlight three major lithological units: 1) a volcano-plutonic unit, formed by gabbros and amphibole-pyroxenite, basalt and rhyodacite; 2) a volcano-sedimentary unit containing pyroclastites (of basaltic and andesitic composition); 3) a sedimentary unit (meta-sedimentary). These rocks are affected by a general metamorphism of green schist facies and a hydrothermal alteration with pervasive and vein alteration marked by the presence of quartz, calcite, epidote, chlorite and sericite. From a geochemical point of view, the results obtained indicate that the plutonites are gabbros while the volcanites and volcanosedimentary rocks have compositions of basalts, basaltic andesites, rhyolites and dacites. They have mainly a tholeitic character related to subduction zones with crustal contamination. The metasediments are arenites emplaced in an active continental margin environment.

Keywords

Petrography, Geochemistry, Petrogenetics, Gouméré-Iguéla, Côte d'Ivoire

1. Introduction

The Paleoproterozoic domain (2.5 to 1.6 Ga), forms part of the West African craton. It consists of juvenile continental Paleoproterozoic crust that was emplaced during the Eburnian orogeny, probably due to oceanic material [1] [2] [3] [4], with an inheritance from older Archean crustal rocks [5]. It consists of belts of Birimian greenstone associated with granitoids [6] [7] [8] [9] [10]. Most of these Birimian formations of the Man Dorsal, about 35%, are found in Côte d'Ivoire and are divided into 17 volcano sedimentary belts, including the Bui belt. The Gouméré region is located in the northeast of Côte d'Ivoire. In the southern part of this region, geological formations attributed to the Tarkwaïan and associated formations are encountered [11] [12] [13] [14]. They are located in the Bui belt, a greenstone belt of Paleoproterozoic age, which extends to north-western Ghana. These have been studied and mapped petrographically using indirect applied geophysical methods [12] [15]. However, the need for further studies is necessary to appreciate their petrographic and geochemical characteristics in more detail. Given the interest of the Tarkwaïan in Ghana, both scientifically and economically, it was necessary to look at the latter in Côte d'Ivoire. It is in this perspective that our study entitled, petrogenetic characterization of the geological formations of the localities of Gouméré-Iguéla. The main objective of this study is to contribute to the improvement of the knowledge on the geological formations of this region in order to deepen for an adequate exploitation of the previous works, on the basis of petrographic and geochemical data.

2. Geological Setting

Côte d'Ivoire belongs to the West African craton and more particularly to the Man Ridge (**Figure 1**). Two geological complexes cover the entire surface of Côte d'Ivoire. A narrow coastal sedimentary basin bordering the Gulf of Guinea that occupies 2.5% of the Ivorian territory and extends from Fresco in the west to Axim in Ghana, and a Precambrian and Crystallophyllous basement that covers the rest of the Ivorian territory, *i.e.* 97.5%. It consists of the Archean and Proterozoic domains. The Archean domain is located west of the Sassandra Fault (**Figure 1**), and is circumscribed within a curve that passes through the SW-NE trending Monts Trou Fault, which marks the southern Sassandra Fault as far as Odienné. This fault continues towards the WNW, in the direction of Guinea. It was structured during two major orogenic cycles: the Leonian (3.4 Ga to 3.0 Ga) and the Liberian (2.9 Ga to 2.7 Ga) [17] [18] [19] [20] [21]. These ages were obtained from radiometric dating performed on the formations in this domain. The Liberian orogeny, which is the most described, is represented by gneisses, amphibole-pyroxenites, iron formations, and coarse-grained ferruginous quartzites. The aluminous gneisses, amphibole-pyroxenites, and ferruginous quartzites are supracrustal rocks that were transformed by catazonal metamorphism during extensive folding [22]. The Liberian plutonic rocks are of intracrustal origin and are represented by a complex of basic and ultrabasic rocks in the Man

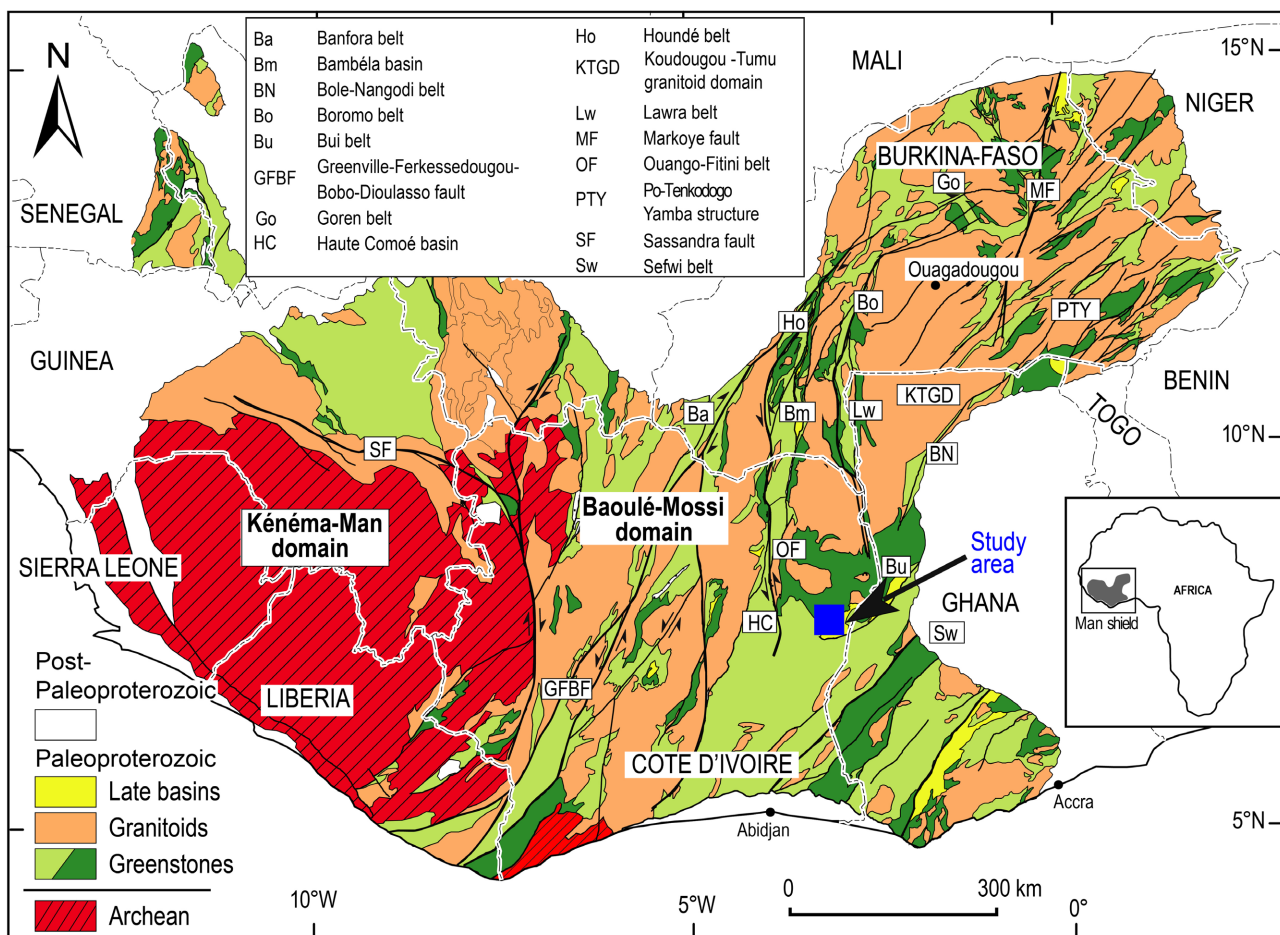


Figure 1. Simplified geological map of the Man-Leo Rise (modified after [16]).

area, migmatites, charnockites and granites associated with migmatites [22] [23]. The Paleoproterozoic domain, located east of the Sassandra Fault, covers the rest of the Ivorian basement. The structuring of this domain has been the subject of several studies, the results of which have been controversial. Indeed, according to some authors [17] [24] and [25], this structuring took place during the Eburnian megacycle (2.5 to 1.6 Ga) and the main tectono-metamorphic phenomena occurred between 2.2 Ga and 2.0 Ga [26]. On the other hand, other authors such as [27] speak of a structuring in two orogenic cycles: the Burkinian (2.4 to 2.15 Ga) and the Eburnian in the strict sense (2.15 to 1.6 Ga).

Reference [2] defines the entire Paleoproterozoic domain as Birimian in age. The Birimian formations form generally NNE-SSW trending volcano-sedimentary sets bordered by or containing granitoids. Seventeen Birimian belts distributed over two fundamental reference alignments, Tehini-Dimbokro (east) and Ferké-Soubré (center), have been identified in Côte d'Ivoire [17] [28]. These belts are composed of metavolcanites, plutonites and metasediments. The Birimian is considered to be formed by a combination of volcanic, subvolcanic and sedimentary rocks emplaced in intracratonic basins. The content of these basins or belts is interpreted by some authors [11] [29] as greenstone belts or volca-

no-sedimentary basins. According to [30], the Birimian belts are subdivided into Type I units (units that were deposited in deep basins and include various formations (Fetékro unit, [31], Aboisso unit) and Type II units that were deposited in shallow basins composed of acidic or intermediate formations and volcano-sedimentary (Bondoukou unit, Dimbokro unit). The area under study is located in the Paleoproterozoic domain (**Figure 1**). It is covered by a complex set of Quaternary and Birimian geological formations. The Birimian occupies virtually the entire surface of the study area and is subdivided into three geological units: the Tarkwaian [11] [13] [32], the volcano-sedimentary and the intrusive [33] (**Figure 2**). This area belongs to the Comoé Birimian sedimentary basin. This basin is one of the largest in the Paleoproterozoic domain and outcrops in Burkina Faso and Ghana in addition to Côte d'Ivoire. The sedimentary basins are mainly siliciclastic, composed of grauwackes and turbiditic argillites, the latter being occasionally carbonated [11] [12] [13] [14]. In addition to these outcrops, some sedimentary basins may also contain significant amounts of volcanoclastics, as well as subordinate volcanic rocks. The geological units of the Comoé basin form a terrigenous sedimentary series comprising phyllitic matrix sandstones, arkoses and pelitic layers, intruded by granitoid massifs and then metamorphosed under greenschist to amphibolite facies conditions [33] [34].

3. Methodology

The study of the geological formations of the Gouméré-Iguéla region consisted

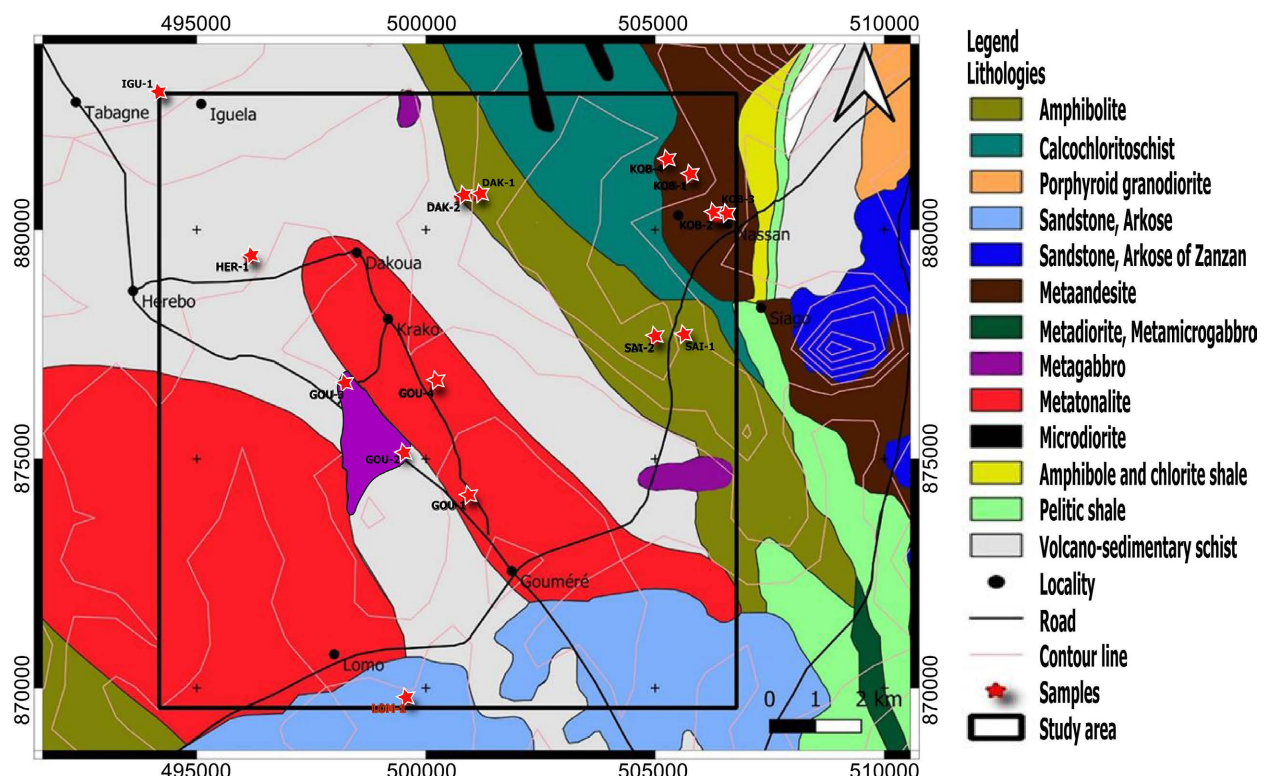


Figure 2. Geological map of Gouméré area with location of analyzed samples (modified after [34]).

of meticulous sampling in the field followed by laboratory work combining different analytical techniques including petrography (macroscopic and microscopic) and lithogeochemistry. Fifteen (15) representative rocks were sampled, followed by the preparation of thin sections and geochemical analyses (**Figure 2**). The thin sections and their microscopic description were carried out at the Laboratory of Geology Mineral Resource and Energetic (LGRME) of University Félix Houphouët-Boigny of Abidjan-Cocody. Geochemical analyses on whole-rock were carried out by Bureau Veritas (Vancouver). In practice, major elements were analyzed by X-ray fluorescence using an XRF while REEs and trace elements were tested by inductively coupled plasma-mass spectrometry (ICP-MS) using an Agilent 7700 \times mass spectrometer. These elements were dosed according to the LF600 package (LF700-LF100-AQ200). These data were processed by computer programs on Excel to establish the normative compositions and the CIPW standard. Then, the GCD kit 4.2 [35] software and the Capdavilla computer program were used to establish the lithogeochemical characterisation diagrams.

4. Results

4.1. Petrography

4.1.1. Plutonites

1) Gabbro

Gabbros are the most dominant lithology in the study area. They are found in the localities of Gouméré, Dakoua, Siago and Kobono. They are melanocratic, massive in appearance (**Figure 3(a)**). Microscopic study of these rocks shows gritty to microgranular porphyritic textures (**Figures 3(b)-(e)**).

- Plagioclase: it represents 25% to 30% of the matrix with rarely automorphic forms. It often occurs in phenocrysts (1 to 2 mm long and 1 mm wide). It is almost unrecognizable on some sections because of alteration. It alters mainly to sericite and damourite and sometimes to epidote. Plagioclase is found in places in inclusion in the green hornblendes. It also shows two types of moles: the polysynthetic mole and the simple or Carlsbad mole. It sometimes shows a zonation characterized by concentric contours around the mineral and suggesting several episodes of magmatism.
- Pyroxene: abundant 35% to 40% in some thin sections and less in others where we have observed an almost total ouralitization in amphibole. Several types of pyroxenes have been described, they are augite showing a macle of albite (**Figure 3(e)**), and hypersthene.

We note that it is sometimes in micrograin associated with quartz in the quartzo-feldspathic veinlets that cross the rock.

- Green Hornblende: it represents 20%, in general xenomorphic and rarely automorphic. This hornblende is millimetric to centimetric, very pleochroic (dark green to light green). It is omnipresent in some parts of the thin section and comes essentially from the ouralitization of pyroxenes. It is presented in

phenoblasts of more or less elongated shape (up to 2 mm long and 1 mm wide) with two sections: a basal section with two cleavage planes making 120° and a longitudinal section. We also note the presence of apatite in inclusion. It is weakly altered in epidote and chlorite (**Figure 3(b)**, **Figure 3(c)**).

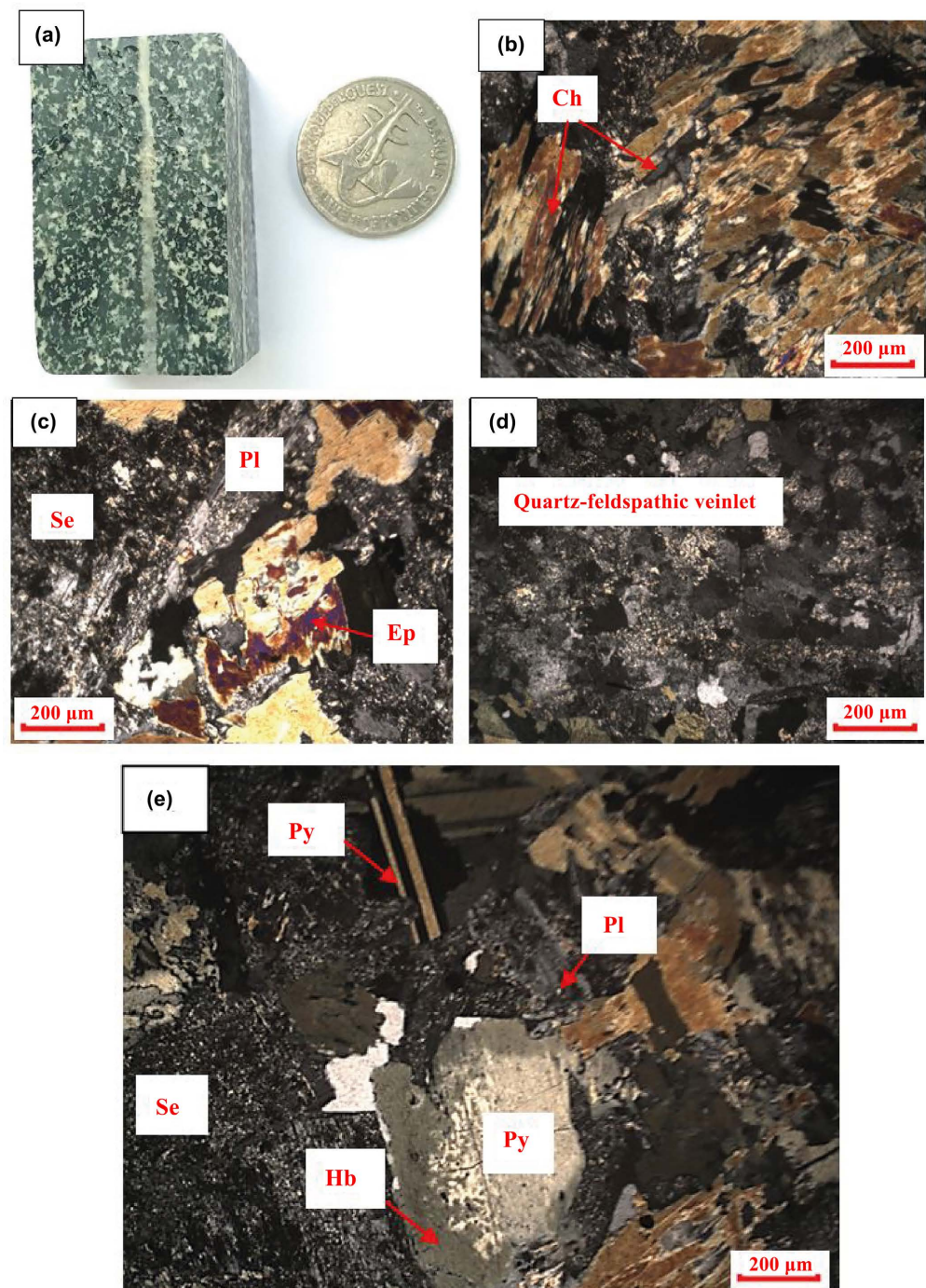


Figure 3. Macroscopic et microscopic aspects of gabbros. (a) Macroscopic aspect; (b) Chloritization; (c) Sericitization and epidotization; (d) Quartz-feldspathic veinlet; (e) Phenocrystal of hornblende. (Py: pyroxene, Pl: plagioclase, Ch: chlorite, Hb: green hornblende, Ep: epidote, Se:sericite).

2) Amphibole-pyroxenite

They are found in the locality of Hérebo. They are melanocratic, of massive aspect (**Figure 4(a)**). Microscopically (**Figure 4(b)**, **Figure 4(c)**), the rock presents a gritty to gritty porphyroid texture composed only of well individualized minerals of pyroxenes and amphibole with a habitus sometimes elongated or prismatic.

- Amphibole: abundant, 45% to 50%, xenomorphic often in automorphic section, greenish with intense pleochroism. It sometimes alters into chlorite and epidote.
- Pyroxene: abundant 40% to 45% of the rock. Two orthogonal cleavage planes are observed in basal section (**Figure 4(d)**). Clinopyroxenes and orthopyroxenes, in this case augite with an extinction angle around 43° and simple macles and the less colored hypersthene are encountered.

4.1.2. Volcanites

1) Basalt

The basalt is of massive or deformed aspect (**Figure 5(a)**). It is generally melanocratic (blackish) and sometimes traversed by veins and veinlets of quartz and calcite. This rock of basaltic composition has been observed in the Kobono and Siago localities. Under the microscope, the basalt has a microlitic porphyry texture (**Figure 5(b)**). The phenocrysts observed are generally pyroxene.

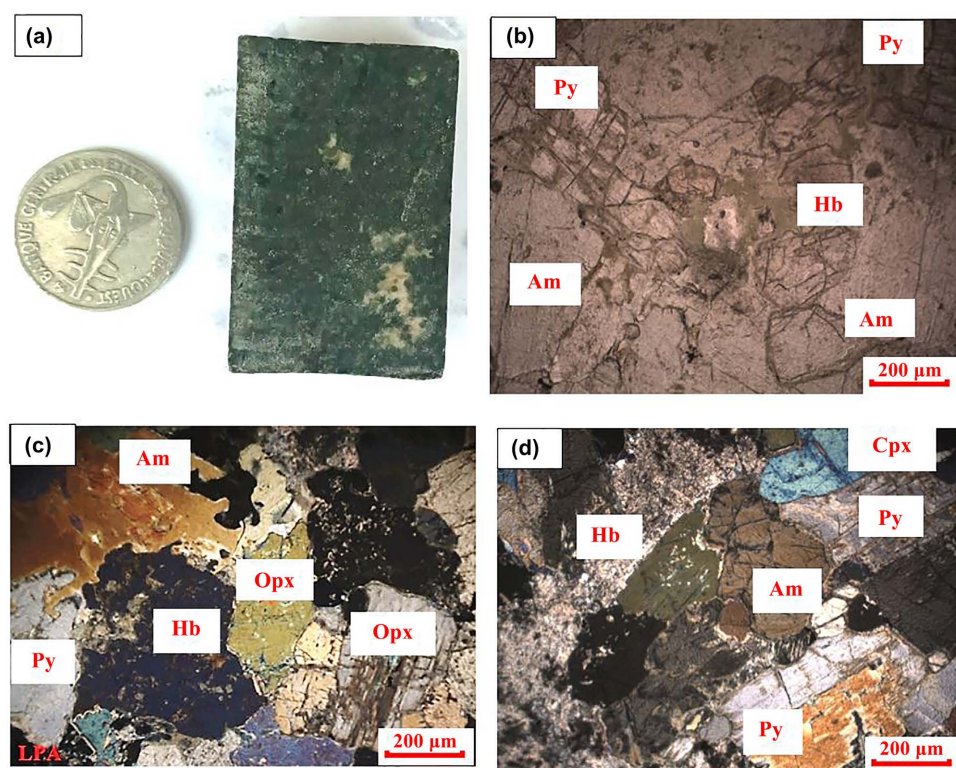


Figure 4. Macroscopic et microscopic aspects of amphibole-pyroxenite. (a) Macroscopic aspect; (b, c, d) Granular texture in thin section. (Py: pyroxene, Opx: orthopyroxene, Cpx: clinopyroxene, Hb: green hornblende, Am: amphibole).

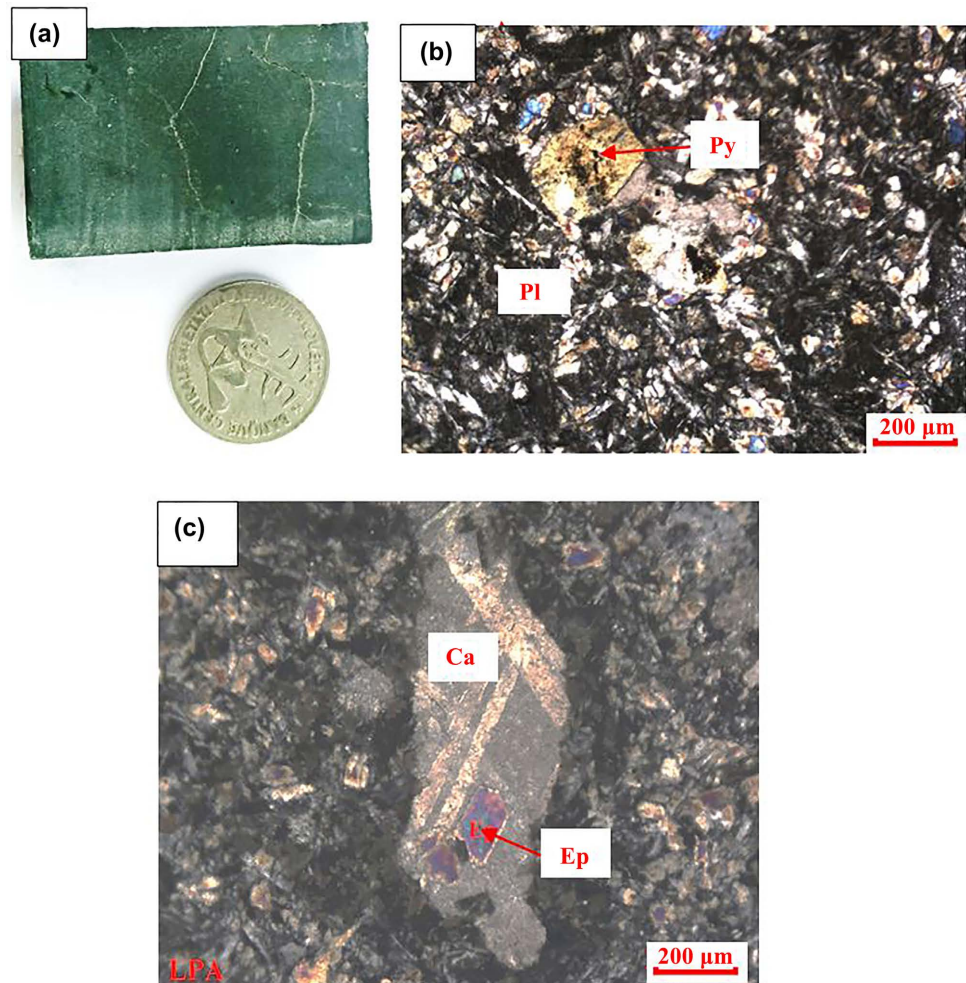


Figure 5. Macroscopic et microscopic aspects of basalt. (a) Macroscopic aspect; (b) Pyroxene phenocrystal in thin section; (c) Calcite and epidote in thin section. (Py: pyroxene, Pl: plagioclase, Ca: calcite, Ep: epidote)

- Green Hornblende: abundant, occurs in microliths and often alters to epidote.
- Pyroxenes: not very abundant, automorphic most often in phenocrysts with two cleavage planes at 90° , most often augite.
- Mesostasis: composed of plagioclase and amphibole rods, is devitrified and partially recrystallized into epidote and sericite minerals.

Carbonate veinlets are also observed, most often associated with epidote, oxides and sulfides (**Figure 5(c)**).

2) Volcanoclastite

These outcrops are located in the locality of Kobono. These rocks are melanocratic. Facies with dark minerals (amphiboles and pyroxenes) of millimeter to centimeter size are the most numerous. These occur locally as breccias and lapilli tuffs (**Figure 6(a)**). Microscopically, we observe a microlithic texture generally destabilized in carbonates and also phenocrysts of quartz and carbonate (**Figure 6(c)**).

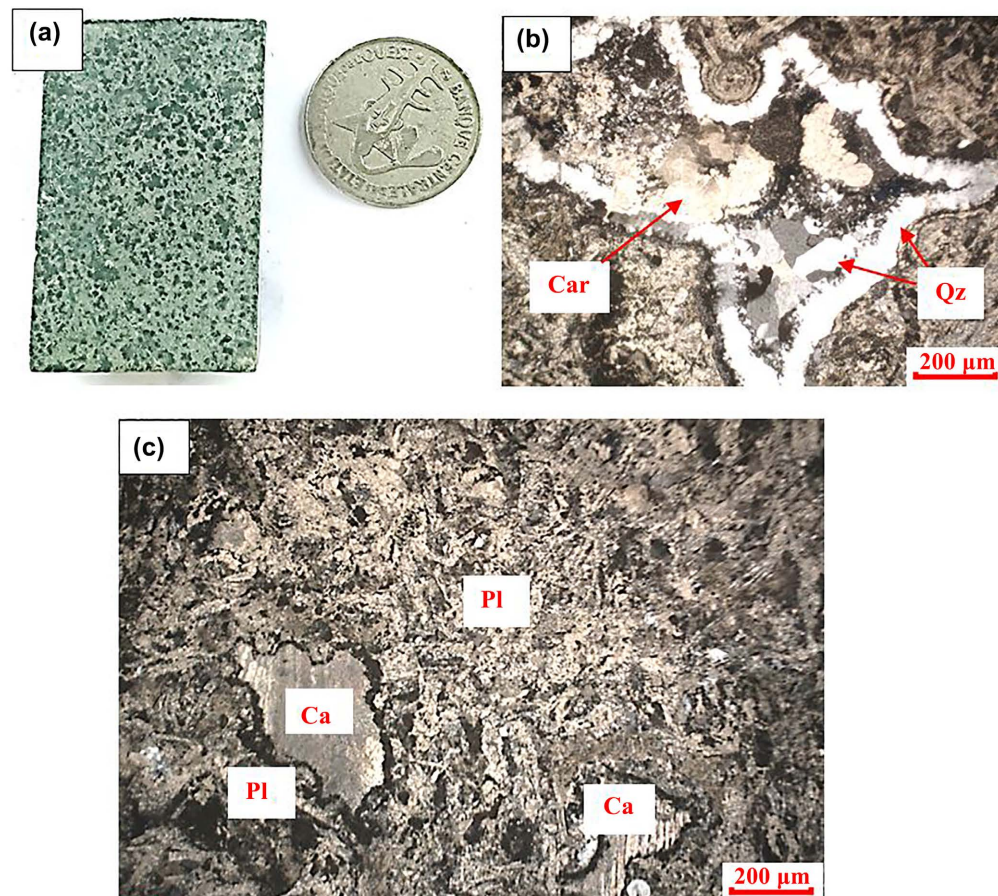


Figure 6. Macroscopic et microscopic aspects of volcanoclastite. (a) Macroscopic aspect; (b) Chalcedony. (Pl: plagioclase, Ca: calcite, Car: carbonate, Qz: quartz)

- Mesostasis: contains glass and minerals of carbonates, sericite and quartz. We also note the presence of quartz-carbonate veinlets. The clasts are mainly composed of chalcedony and carbonate.
- Chalcedony: subautomorphic to automorphic, consists of a quartz crown, there are two generations of quartz depending on their size and carbonates (**Figure 6(b)**).
- Carbonates: mainly subautomorphic calcite, recognizable by its Carlsbad macle.

3) Rhyodacite

These outcrops are located in the Kobono locality. These rocks are mesocratic (brownish) with dark minerals (amphiboles) of millimeter to centimeter size being the most numerous. Quartz phenocrysts are also present (**Figure 7(a)**). The microscopic mineralogy of the rhyodacites shows a porphyritic microlithic texture, composed of plagioclase, amphibole and quartz in a plagioclase matrix.

- Plagioclase: abundant and automorphic (rectangular), sometimes in phenocrysts up to 1.5 mm long and 1 mm wide. It may exist as a micrograin associated with the matrix. It is frequently altered to sericite and sometimes shows zonation (**Figure 7(b)**).

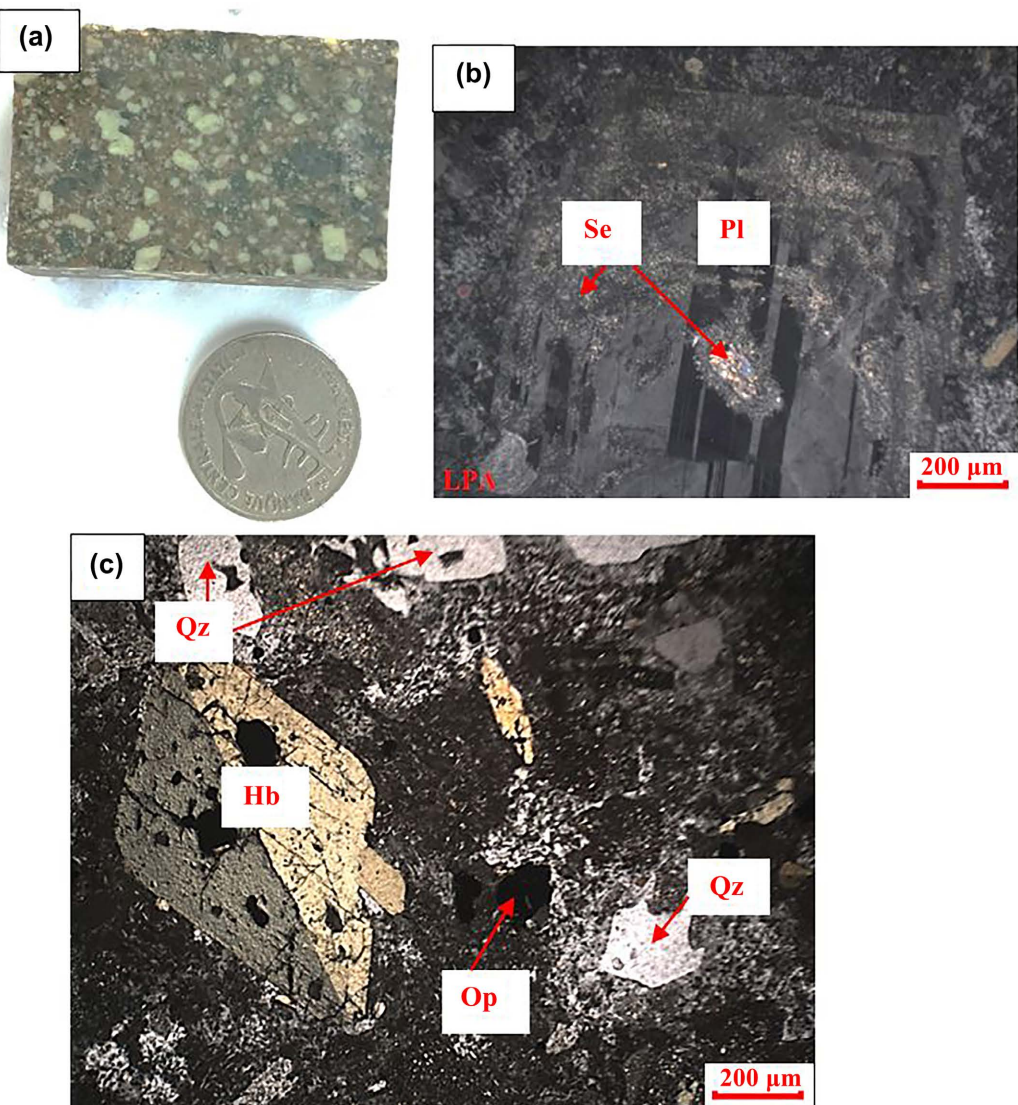


Figure 7. Macroscopic et microscopique aspects of rhyodacite. (a) Macroscopic aspect; (b), (c) Microscopic aspect. (Pl: plagioclase, Se: sericite, Hb: green hornblende, Qz:quartz, Op: opaque).

- Amphibole: automorphic (rhombic) phenocrysts of about 1.5 mm long and 1mm wide. It has two cleavage planes at 120° in basal section. It also exists in automorphic micrograin (**Figure 7(c)**).
- Quartz: less abundant, subautomorphic, corroded and showing rolling extinction.
- Mesostasis is essentially composed of plagioclase microliths, showing a sericitization.

4.1.3. Micro-Conglomerate

These rocks were collected in the localities of Lomo and Iguéla, of brown color, they are characterized by grains of quartz taken in a clayey cement (**Figure 8(a)**). Microscopy reveals quartz and muscovite minerals organized in a granular texture (**Figure 8(b)**, **Figure 8(c)**).

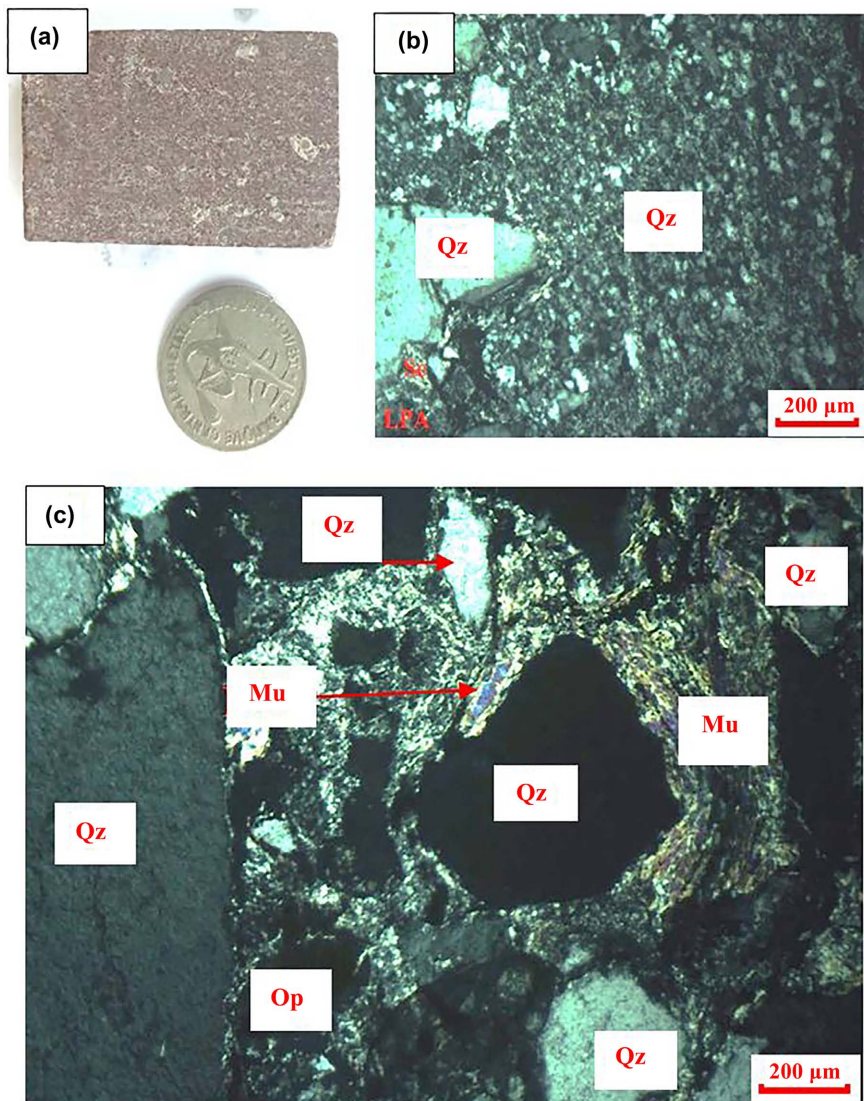


Figure 8. Macroscopic et microscopic aspects of micro-conglomerate. (a) Macroscopic aspect; (b) (c) Microscopic aspect. (Mu: muscovite, Qz: quartz, Op: opaque)

- Quartz: very abundant, 70% to 80% of minerals. It is subrounded and angular with a diameter of up to 1 mm. It is often in the form of cracked porphyroblasts showing a direction of deformation and also in micro grains (**Figure 8(c)**). These grains have a preferential orientation.
- Muscovite: rare, showing a wavy extinction and a bright hue. It is found only in the matrix.
- Matrix: less than 20%, it is made of ferro-titanium clay with an important sericitization.

4.2. Geochemistry

Major element (wt%) chemical analyses (**Table 1**) of the samples are projected onto discriminant diagrams to establish the classification and nomenclature of all the rocks.

Table 1. Major element composition (%) of the samples collected.

Samples	GOU 1	GOU 2	GOU 3	GOU 4	KOB 1	KOB 2	KOB 3	KOB 4
	Plutonic	Plutonic	Plutonic	Plutonic	Volcanic	Plutonic	Volcano-clastic	Volcanic
SiO ₂	49.38	54.2	52.27	48.72	52.57	49.86	50.14	67.02
TiO ₂	0.85	0.93	0.75	0.8	1.01	1.37	0.81	0.42
Al ₂ O ₃	16.66	15.31	14.75	13.75	14.57	14.08	12.85	15.02
Fe ₂ O ₃	9.72	11.19	9.79	14.22	11.69	14.59	8.84	4.63
MnO	0.14	0.15	0.16	0.22	0.21	0.22	0.16	0.07
MgO	6.31	5.29	9.07	7.36	6.41	5.61	3.61	1.51
CaO	10.39	8.08	9.03	11.3	7.85	9.07	10.01	3.3
Na ₂ O	3.11	3.29	2.25	1.95	4.09	2.76	2.32	5.28
K ₂ O	0.74	0.45	0.8	0.18	0.21	0.4	0.38	1.06
P ₂ O ₅	0.11	0.14	0.11	0.06	0.11	0.07	0.09	0.11
Cr ₂ O ₃	0.04	0.03	0.07	0.03	0.04	0.01	0.05	0.02
LOI	1.42	1.08	1.58	2	2.04	2.8	10.98	0.79

Samples	DAK 1	DAK 2	SAI 1	SAI 2	LOM 1	HER 1	IGU 1
	Plutonic	Plutonic	Volcanic	Plutonic	Micro-conglomerate	Plutonic	Micro-conglomerate
SiO ₂	49.11	50.75	78.38	52.03	80.32	52.78	86.14
TiO ₂	1.9	0.78	0.25	1.25	0.46	0.33	0.22
Al ₂ O ₃	14.87	16.06	10.39	13.11	8.99	4.03	6.23
Fe ₂ O ₃	15.15	10.21	3.03	14.19	5.63	11.07	3.62
MnO	0.16	0.15	0.22	0.23	0.03	0.21	0.02
MgO	5.27	7.29	2.54	5.69	0.39	17.31	0.29
CaO	9.04	10.52	0.26	9.76	0.09	13.08	0.07
Na ₂ O	2.53	2.66	1.92	2.65	0.12	0.55	0.12
K ₂ O	0.38	0.4	0.44	0.22	2.63	0.33	1.82
P ₂ O ₅	0.07	0.05	0.13	0.08	0.04	0.01	0.03
Cr ₂ O ₃	0.03	0.07	0.01	0.01	0.02	0.09	0.01
LOI	1.6	2.12	2.53	1.74	1.34	1.04	0.64

4.2.1. Plutonic Rocks

These rocks (GOU, DAK, KOB 2, SAI 2, HER 1) are characterized by SiO₂ contents of 48.72% to 54.2% and alkalis (Na₂O + K₂O) of 2.85% to 3.87%, which give them a gabbro and gabbroic diorite composition on the classification diagram of [36], (Figure 9). Al₂O₃ contents vary between 13.11% and 16.66%; MgO between 5.29% and 9.07%; Fe₂O₃ between 9.72% and 15.15%. CaO contents vary from 8.08% to 11.3%, Na₂O from 1.95% to 3.29% and K₂O from 0.18% to 0.8%. MnO contents are between 0.14% and 0.23%. The TiO₂ values are lower than 2%. Amphibole-pyroxenites (HER 1) show SiO₂ contents of 67.02; MgO of 17.31%;

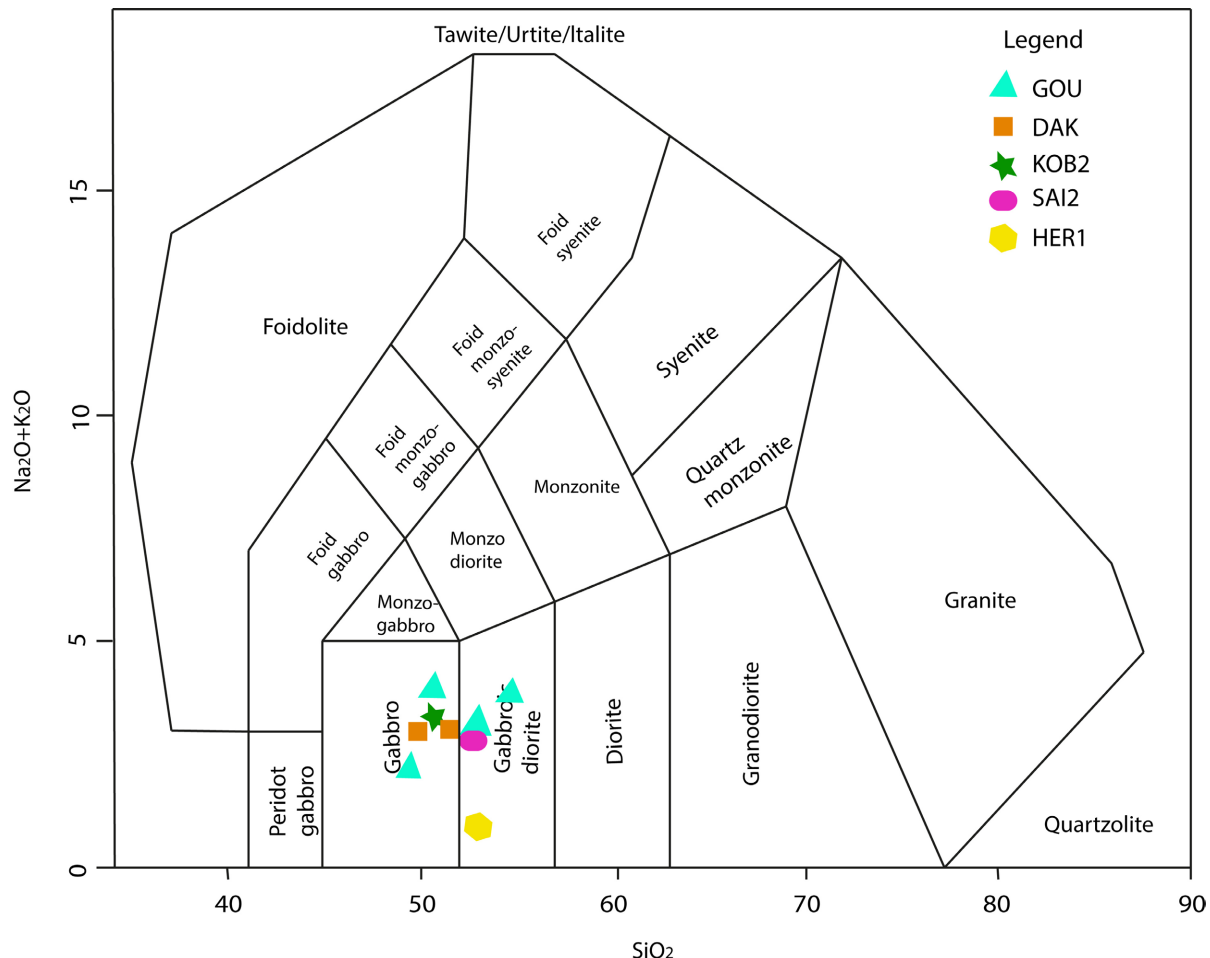


Figure 9. TAS diagram after [36] applied to analyzed plutonic samples.

Fe_2O_3 of 11.07%; Al_2O_3 of 4.03% and CaO of 13.08%. Na_2O contents of 0.55%; K_2O of 0.33%; MnO of 0.21%. TiO_2 values are less than 2% (0.33%), (**Table 1**). They have a tholeiitic series (**Figure 10**).

4.2.2. Volcanic Rocks

The basalt (KOB 1), (**Figure 11**) has SiO_2 contents of 52.57% (**Table 1**); MgO of 6.47%; Fe_2O_3 is 11.69%; Al_2O_3 of 14.57% and CaO of 9.07%. Na_2O and K_2O contents are 4.09% and 0.21% respectively. The low TiO_2 content of 1.37% of the analyzed basalt resembles those of plutonic rocks of magmatic arcs [38], but are different from intraplate basalts, which often possess high TiO_2 contents (>2%).

This mafic volcanoclastite (KOB 3) is characterized by SiO_2 contents of 50.14% (**Table 1**); MgO of 3.61%; Fe_2O_3 of 8.84%; Al_2O_3 of 12.85% and CaO of 10.01%. Na_2O and K_2O contents vary respectively by 2.32% and 0.38%; MnO by 0.16%. Low levels of TiO_2 (0.81%) are also observed. This rock corresponds to basaltic andesites as shown in the diagram of [36], (**Figure 11**).

Rhyodacite (KOB 4) shows SiO_2 contents of 67.02%; MgO of 1.51%; Fe_2O_3 of 4.63%. Al_2O_3 varies by 15.02%; CaO by 3.3%; Na_2O by 5.28%; K_2O by 1.06% and MnO by 0.07%. TiO_2 values are less than 2% (0.42%).

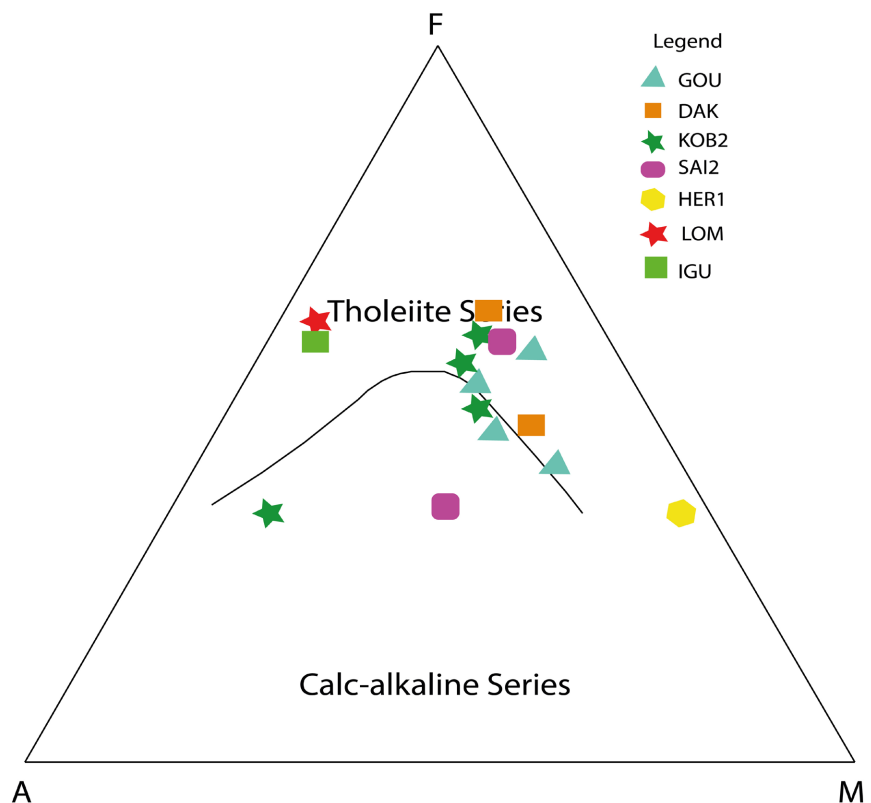


Figure 10. AFM diagram [37] applied to plutonites and volcanites of the Gouméré region.

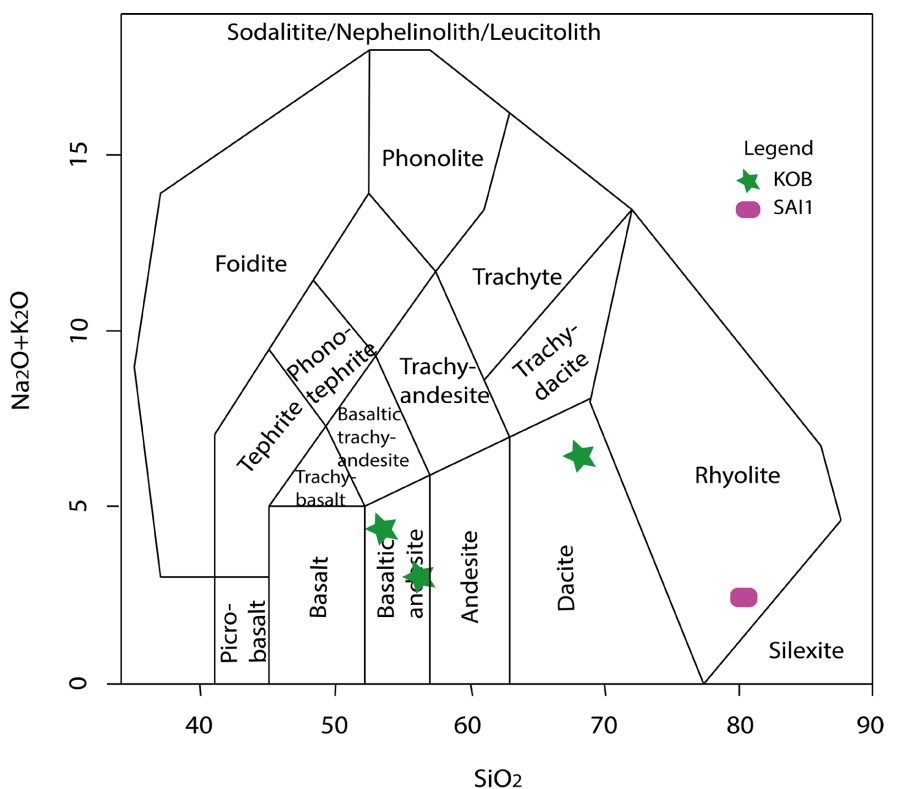


Figure 11. TAS diagram after [36] applied to analyzed volcanic samples.

In the diagram of [37] (Figure 10), these formations generally have a tholeiitic composition.

4.2.3. Micro-Conglomerate

The diagram of [39] which makes it possible to discriminate the rocks of magmatic and sedimentary origin has allowed us to highlight two samples of sedimentary origin: IGU 1 and LOM 1 (Figure 12). This diagram is based on the P_2O_5/TiO_2 ratios as a function of MgO/CaO . These ratios give values for sandstones (micro-conglomerate) between 0.09 - 0.14 for P_2O_5/TiO_2 and 4.14 - 4.33 for MgO/CaO .

Reference [40] diagram based on $\log(SiO_2/Al_2O_3)$ and $\log(Fe_2O_3/K_2O)$ ratios, values range from 0.8 - 1.1 and 0.47 - 0.54 shows a litharenite and sublitharenite composition respectively for the IGU 1 and LOM 1 samples (Figure 13).

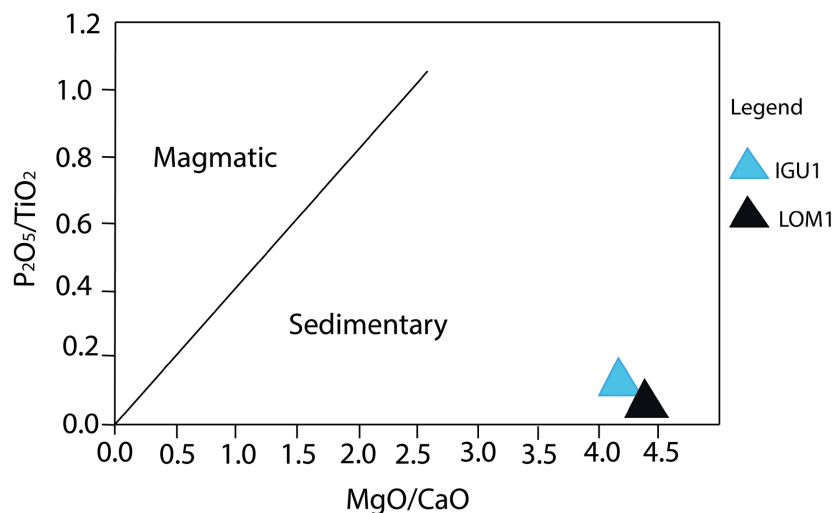


Figure 12. P_2O_5/TiO_2 versus MgO/CaO diagram of [39] applied to micro-conglomerate.

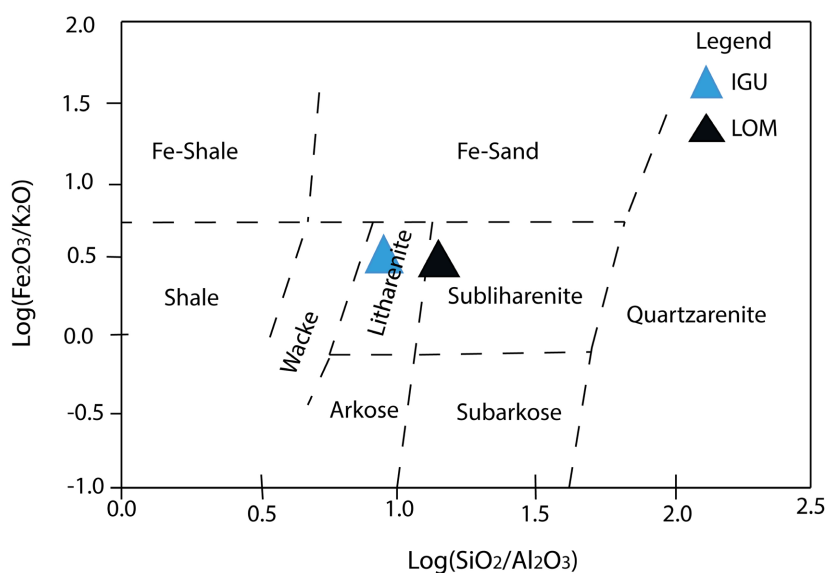


Figure 13. Diagram of [40] applied to micro-conglomerate.

4.3. Petrogenesis

Trace element chemical analyses (**Table 2** and **Table 3**) of the samples are projected onto ternary and binary discriminant diagrams to establish the geodynamic context of emplacement.

Table 2. Trace element composition (ppm) of collected samples.

Samples	GOU1	GOU2	GOU3	GOU4	DAK1	DAK2	KOB1	KOB2
	Plutonic	Plutonic	Plutonic	Plutonic	Plutonic	Plutonic	Volcanic	Plutonic
Ba	408	156	408	61	121	123	111	145
Be	<1	<1	<1	<1	<1	<1	<1	<1
Co	40.2	42.9	51.3	59.3	49.2	42.5	48.6	48.6
Cs	0.5	0.6	1.2	0.3	0.2	0.2	<0.1	0.3
Ga	18.0	18.8	11.6	14.5	18.2	14.3	11.9	16.9
Hf	1.7	1.6	1.7	1.2	1.7	1.0	1.7	1.8
Nb	3.5	2.2	5.0	2.1	3.0	1.6	1.8	2.5
Rb	16.2	8.6	20.8	5.1	10.7	13.5	6.8	9.1
Sn	<1	<1	<1	<1	<1	<1	<1	<1
Sr	458.1	382.6	252.1	101.8	417.8	389.4	278.0	181.6
Ta	0.2	<0.1	0.2	<0.1	0.1	<0.1	0.1	0.2
Th	0.3	1.1	0.7	<0.2	1.0	0.4	<0.2	0.5
U	0.1	0.3	0.4	<0.1	0.2	0.2	<0.1	0.2
V	230	178	162	288	251	152	279	392
W	0.8	3.2	0.9	0.6	0.8	<0.5	0.7	<0.5
Zr	65.4	53.7	63.7	38.8	56.9	31.6	55.9	56.0
Y	16.9	14.4	15.0	20.3	13.0	9.2	23.1	20.2
La	10.7	11.3	8.1	1.7	8.2	5.4	3.2	5.5
Ce	18.0	25.2	18.4	4.2	18.3	12.2	7.7	11.9
Pr	3.17	3.34	2.51	0.69	2.50	1.66	1.30	1.59
Nd	14.2	15.2	11.5	4.3	12.2	7.9	6.8	7.7
Sm	3.11	3.43	2.46	1.55	2.94	1.94	2.13	2.26
Eu	1.10	1.15	0.88	0.74	1.13	0.74	0.85	0.89
Gd	3.38	3.35	2.66	2.64	3.07	2.03	3.25	3.17
Tb	0.55	0.51	0.44	0.52	0.49	0.30	0.57	0.53
Dy	3.30	2.82	2.41	3.35	2.76	1.79	3.78	3.57
Ho	0.69	0.59	0.53	0.82	0.50	0.36	0.85	0.74
Er	1.98	1.66	1.61	2.50	1.43	1.00	2.68	2.10
Tm	0.30	0.22	0.23	0.36	0.18	0.12	0.31	0.29
Yb	1.98	1.39	1.44	2.33	1.14	0.89	2.17	1.84
Lu	0.28	0.19	0.21	0.37	0.18	0.12	0.34	0.26
Se	<0.5	<0.5	<0.5	<0.5	<0.5	<0.5	<0.5	<0.5

Table 3. Trace element composition (ppm) of collected samples.

Samples	KOB3	KOB4	SAI1	SAI2	LOM1	HER1	IGU1
	Volcano-clastic	Volcanic	Volcanic	Plutonic	Micro-conglomerate	Plutonic	Micro-conglomerate
Ba	124	333	229	34	334	67	306
Be	<1	2	<1	<1	<1	<1	<1
Co	33.5	12.2	13.7	47.8	12.7	74.8	7.4
Cs	0.2	0.1	0.9	<0.1	4.9	0.7	2.0
Ga	12.7	16.5	11.4	15.9	9.6	5.9	6.6
Hf	1.8	3.5	2.9	2.0	2.9	0.8	1.5
Nb	2.8	5.1	4.6	2.9	4.4	0.6	2.5
Rb	13.0	18.9	10.0	3.3	69.8	13.1	53.1
Sn	<1	<1	<1	1	<1	<1	<1
Sr	166.7	357.3	74.4	122.0	51.4	70.8	43.3
Ta	0.3	0.3	0.3	0.1	0.3	<0.1	0.1
Th	0.4	2.7	3.1	0.2	5.6	0.3	1.7
U	0.1	0.9	0.5	<0.1	0.8	0.1	0.9
V	203	67	25	364	78	182	35
W	<0.5	<0.5	1.8	<0.5	3.8	1.5	1.2
Zr	58.8	134.9	110.7	66.8	110.6	21.6	60.9
Y	15.3	9.5	6.8	24.7	10.7	8.1	8.3
La	4.7	19.0	17.5	8.8	48.1	2.6	38.1
Ce	11.3	37.3	35.5	8.7	100.3	6.1	75.8
Pr	1.50	4.18	4.20	1.40	10.10	0.93	7.75
Nd	7.3	16.3	16.3	7.5	38.0	4.8	26.6
Sm	2.07	2.63	2.65	2.37	6.73	1.22	4.32
Eu	0.75	0.88	0.59	1.02	1.66	0.45	0.99
Gd	2.63	2.25	1.96	3.51	5.23	1.55	2.86
Tb	0.44	0.32	0.26	0.64	0.63	0.24	0.38
Dy	2.82	1.81	1.29	4.16	3.23	1.51	1.72
Ho	0.63	0.35	0.26	0.92	0.52	0.31	0.35
Er	1.85	0.97	0.81	2.67	1.16	0.97	0.81
Tm	0.24	0.13	0.10	0.39	0.15	0.12	0.12
Yb	1.68	0.96	0.70	2.60	1.03	0.73	0.76
Lu	0.25	0.13	0.10	0.40	0.14	0.12	0.12
Se	<0.5	<0.5	<0.5	<0.5	<0.5	<0.5	<0.5

4.3.1. Plutonites

Chemical analyses of the plutonites are highlighted on the (Y + Nb) versus Rb diagram of [41], (Figure 14). It appears that the gabbros show a geochemical

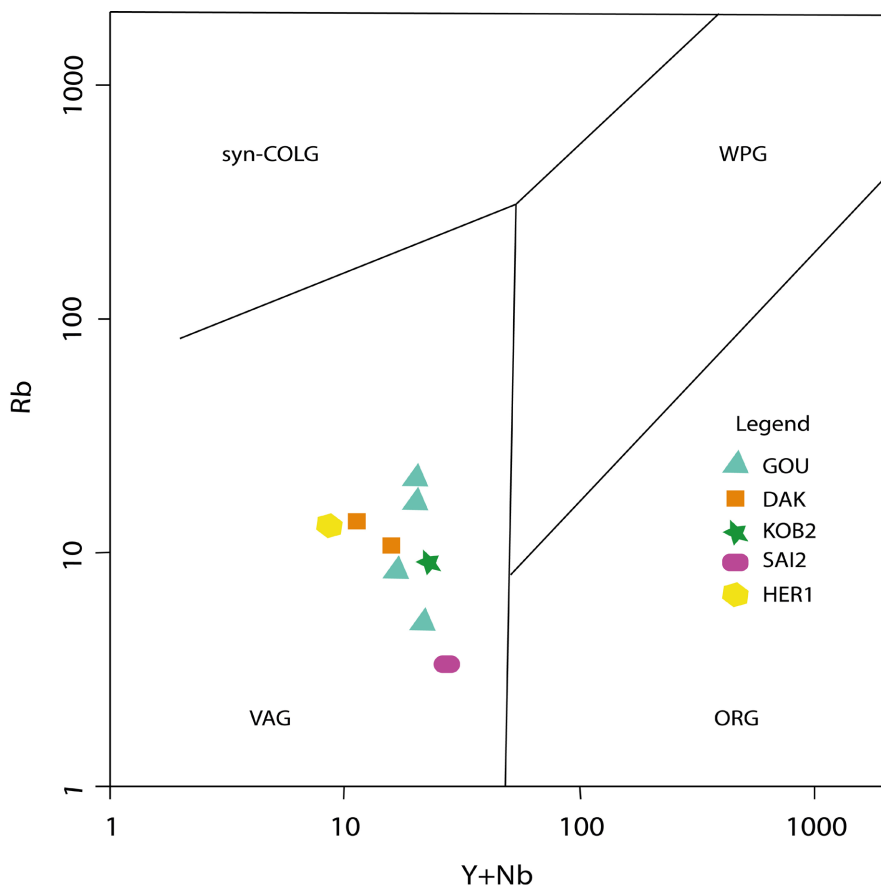


Figure 14. Reference [41] diagram $\text{Rb}/(\text{Y} + \text{Nb})$ applied to plutonites.

signature of volcanic arc (VAG). These gabbros show significant depletion in high potential elements (HFSE) (Nb, Ta, Zr and Hf), low in heavy rare earths (HREE) and positive Eu anomalies (**Table 2** and **Table 3**).

4.3.2. Volcanites

In the diagram of [42] [43], (**Figure 15**), basalts, mafic volcanoclastites, and rhyodacites are found above the mantle row. Given the arrangement of the rocks studied in this diagram, the basic and intermediate metavolcanites are enriched by components of subduction zones or by assimilation of continental crust. From this, we can say that the basic and intermediate volcanics of the study area were contaminated by crustal components during their emplacement. In the Th-Hf-Nb ternary diagram of [44], the mafic volcanic rocks (basalt and andesitic basalt) are emplaced in a context of volcanic arcs, and follow a tholeiitic lineage while the acidic volcanics (rhyodacite) follow a calc-alkaline lineage (**Figure 16**).

4.3.3. Micro-Conglomerate

The SiO_2 -log $(\text{K}_2\text{O}/\text{Na}_2\text{O})$ discrimination diagram of [45] (**Figure 17**) highlights the geotectonic environments of the sediments. The log $(\text{K}_2\text{O}/\text{Na}_2\text{O})$ value of the metasediments is of the order of 0.5 and places them in the field of an active continental margin. The rare earth fractionation rate of the metasediments is

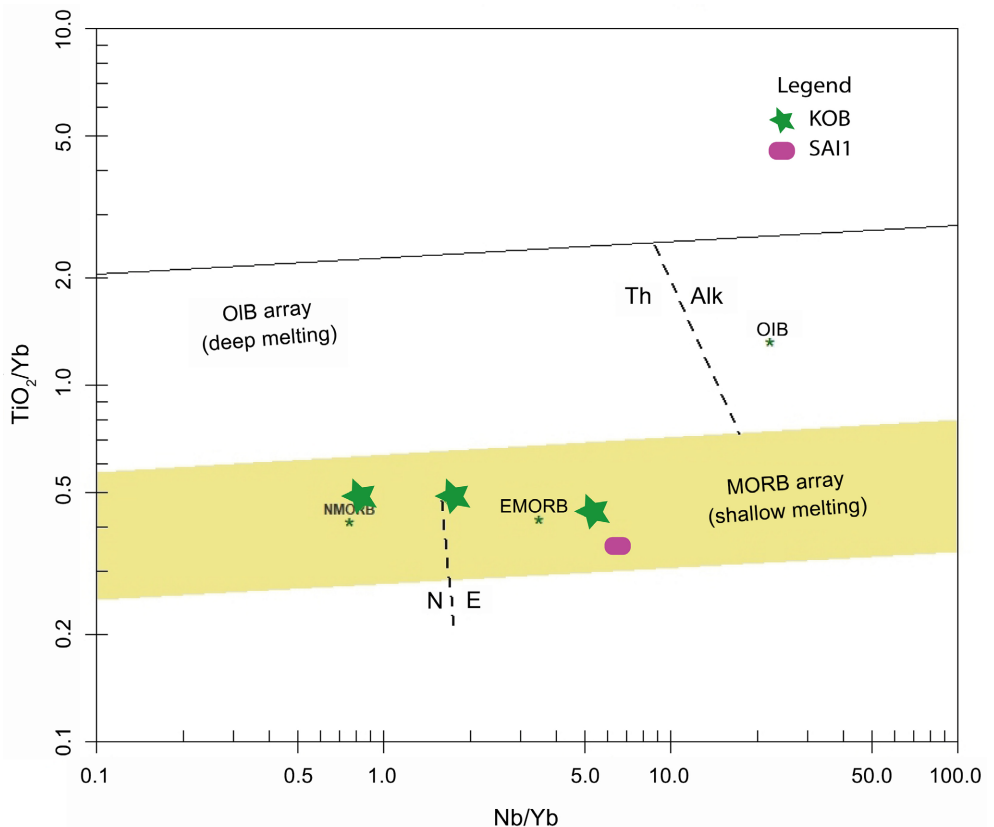


Figure 15. Reference [42] [43] diagram Th/Yb vs Nb/Yb applied to volcanites.

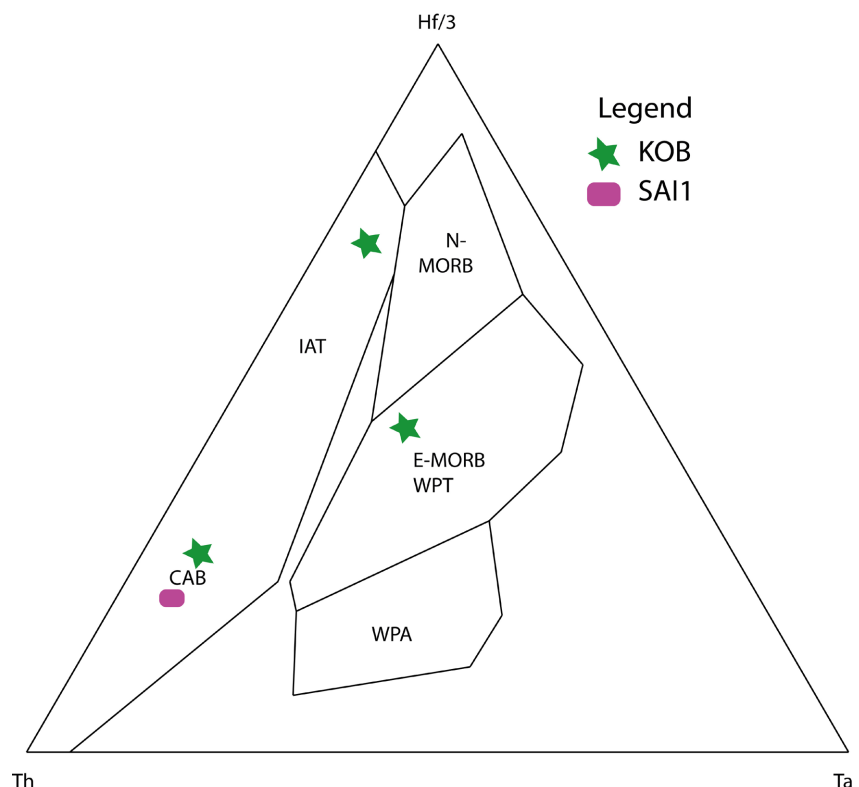


Figure 16. Th-Hf-Nb diagram of [44] applied to volcanites.

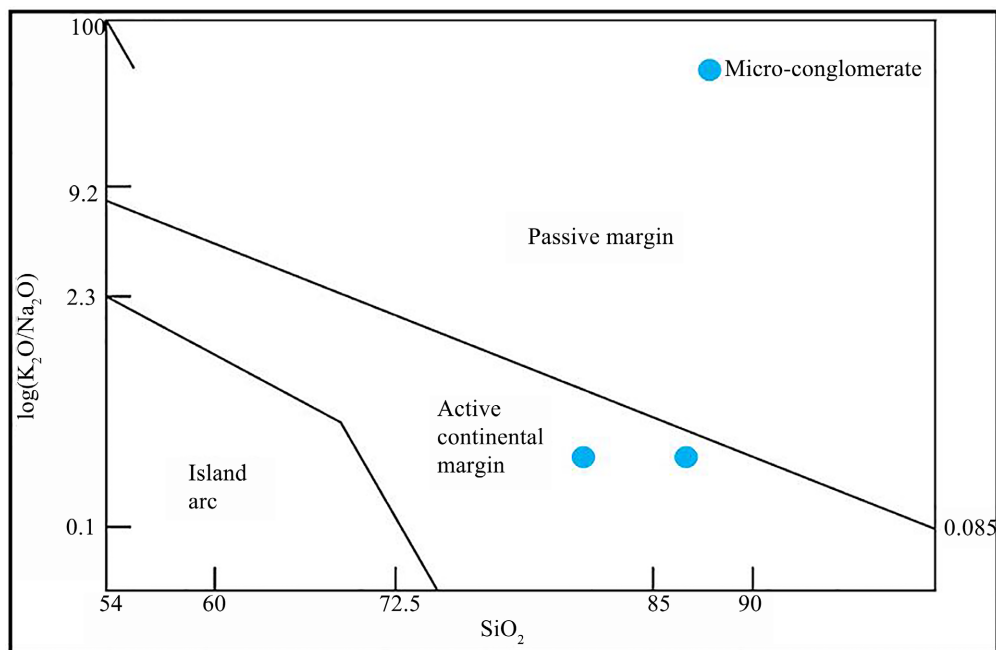


Figure 17. SiO₂-log (K₂O/Na₂O) discrimination diagram of [45] applied to the micro-conglomerate.

generally low, with a marked positive Eu anomaly (0.99 - 1.66). Positive Eu anomalies imply crystallization of plagioclase and alkali feldspar by fractional crystallization or partial melting of the rock.

5. Discussion

The study area is constituted of volcano-plutonites mainly gabbros, amphibole-pyroxenites, basalts and rhyodacites. These formations have also been described by [46] in Ghana and [34] in the study area. This work also reveals the presence of sandstone with quartzite character. This rock is similar to the quartzite described by [46] in the Ghanaian Tarkwaian. The metamicroconglomeratic level with quartz pebbles and phyllite minerals observed at Iguéla is similar to the Banket series described by [46] in the Ghanaian Tarkwaian. These results had been obtained by [11] in the same area. Reference [47] also state that the Tarkwaian in Burkina-Faso consists of sandstone, quartzite, arkose, phyllite and conglomerates (with pebbles from the adjacent greenstone belt: quartz, rhyolite, schist) weakly metamorphosed [48]). The petrographic study showed that the host rocks in the Gouméré area underwent metamorphic and hydrothermal alteration processes. The commonly observed alteration minerals are: sericite, epidote, chlorite and hornblende ± actinote. All these minerals are only low pressure minerals; there are no high pressure minerals. The presence of chlorite, epidote and sericite in the rocks indicates that the area was affected by greenschist facies metamorphism. These metamorphic conditions have been described by [47]. The rocks studied indicate that the lithostratigraphy of the southern Bui Trench is similar to that of most volcanosedimentary trenches of the Baoulé-Mossi domain, except the presence of granitoids in our analyzed samples ([17] [47]).

[49] [50]).

The TAS diagram applied to the plutonites allowed us to highlight gabbros and gabbro-diorites. The volcanics have compositions of basalt, rhyodacite and volcanoclastites with a history of basaltic andesite. These geochemical characters are similar to those described by [31], in the gabbros and basalts of the Agbahou gold deposits, located south of the Fettékro green stone belt. The metasediments were highlighted by the diagram of [40]. These formations give very low TiO_2 contents ranging from 0.05% - 1.71%. This suggests that these are similar to the magmatic arc volcanics described by several authors in the Toumodi Fettékro green stone belt ([51] [52] [53]). Strontium enrichment is indicative of the presence of plagioclase in basalts. Basaltic lavas correspond to arc-volcanic tholeites close to N-MORBs, as suggested by different authors on the Man-Leo Ridge lavas ([1] [2] [31] [51] [54] [55] [56]). According to [57], Ba/Ta ratios greater than 450 and Ba/Nb ratios greater than 28 are the most notable features of magmas related to subduction zones. Volcanites and plutonites show the following Ba/Ta and Ba/Nb ratios: volcanites ($Ba/Ta = 725 - 1110$; $Ba/Nb = 44 - 65$); plutonites ($Ba/Ta = 340 - 2040$; $Ba/Nb = 29 - 117$). This implies that the basic and intermediate volcanics of the study area would originate from a subduction zone as well as the rocks of the Toumodi-Fettékro belt ([31] [53]) and Ashanti belt ([58]). Concerning the acid volcanics, they are composed of rhyodacites. Geochemical data indicate that the acid lavas correspond to arc volcanics. The low Y and high Zr/Y concentrations suggest that these rhyodacites are close to rhyolites ([59]). Indeed, they are generally interpreted as being formed by low-temperature ($<900^{\circ}C$) melts at deep crustal levels (>10 km) ([59] [60]). According to these authors, these melts have low potential to drive hydrothermal systems because of their low melting temperature and heat loss during transport to the crustal surface.

6. Conclusion

The geological formations of Gouméré-Iguéla present a varied geographic and geodynamic context. At the level of petrography, we meet gabbros, basalts, rhyodacite, amphibole-pyroxenite volcanoclastite and metasediments. These lithologies have been generally affected by hydrothermal (pervasive and vein) and meteoric alteration processes. The pervasive alterations observed are chloritization, carbonation, damouritization, sericitization. The vein alteration is summarized in quartz-feldspathic veins and veinlets. These rocks are intensely altered. Uralitization, sericitization, carbonation, epidotization and sulfidation have been observed in most of these lithologies. These alterations are related to hydrothermalism. The metamorphism is mostly greenschist to locally amphibolitic facies. Geochemical data indicate that the magmatic, volcanic and volcanosedimentary rocks have compositions of basalts, basaltic andesites, andesites and rhyodacites. The plutonites are gabbros. The rocks present mainly a tholeitic character related to the subduction zones with a crustal contamination. As for

the metasediments, they are of arenitic type and are emplaced in an active continental margin environment.

Acknowledgements

This work is part of the projects financed by TROPIC MINING GROUP and supported by the Ministry of Higher Education and Scientific Research of Côte d'Ivoire (MESRS).

Conflicts of Interest

The authors declare no conflicts of interest regarding the publication of this paper.

References

- [1] Abouchami, W., Boher, M., Michard, A. and Albarede, F. (1990) A Major 2.1 Ga Event of Mafic Magmatism in West Africa: An Early Stage of Crustal Accretion. *Journal of Geophysical Research: Solid Earth*, **95**, 17605-17629. <https://doi.org/10.1029/JB095iB11p17605>
- [2] Boher, M., Abouchami, W., Michard, A., Albarede, F. and Arndt, N.T. (1992) Crustal Growth in West Africa at 2.1 Ga. *Journal of Geophysical Research: Solid Earth*, **97**, 345-369. <https://doi.org/10.1029/91JB01640>
- [3] Dia, A., Van Schmus, W.R. and Kröner, A. (1997) Isotopic Constraints on the Age and Formation of a Palaeoproterozoic Volcanic Arc Complex in the Kedougou Inlier, Eastern Senegal, West Africa. *Journal of African Earth Sciences*, **24**, 197-213. [https://doi.org/10.1016/S0899-5362\(97\)00038-9](https://doi.org/10.1016/S0899-5362(97)00038-9)
- [4] Pouclet, A., Doumbia, S. and Vidal, M. (2006) Geodynamic Setting of the Birimian Volcanism in Central Ivory Coast (Western Africa) and Its Place in the Palaeoproterozoic Evolution of the Man Shield. *Bulletin de la Société Géologique de France*, **177**, 105-121. <https://doi.org/10.2113/gssfbull.177.2.105>
- [5] Kouamelan, A.N., Peucat, J.J. and Delor, C. (1997) Reliques archéennes (3,15 Ga) au sein du magmatique birimien (2,1 G.a) de Côte d'Ivoire, craton ouest-africain. *Comptes rendus de l'Académie des Sciences*, **324**, 719-727.
- [6] Yacé, I. (1972) Le Birrimien de la région de Toumodi (Côte d'Ivoire). *Annales de l'Université d'Abidjan: Sciences. Série C*, **8**, 27-31.
- [7] Yacé, I. (1977) Contribution à l'étude du volcanisme du protérozoïque inférieur de l'Afrique de l'Ouest: l'Exemple du Centre-Sud-Est de la Côte d'Ivoire. *Bulletin de la Société Géologique de France*, **S7-XIX**, 991-993. <https://doi.org/10.2113/gssfbull.S7-XIX.5.991>
- [8] Milesi, J.P., Feybesse, J.L., Ledru, P., Domanget, A., Ouedraogo, M.F., Marcoux, E., Prost, A., Vinchon, C., Sylvain, J.P., Johan, V., Tegyey, M., Calvez, J.Y. and Lagney, P. (1989) Les minéralisations aurifères de l'Afrique de l'Ouest, leurs relations avec l'évolution lithostructurale au Protérozoïque inférieur Carte au 1/2,000,000eme. *Chronique de la Recherche Minière*, **497**, 3-98.
- [9] Feybesse, J.L., Billa, M., Guerrot, C., Duguey, E., Lescuyer, J.L., Milesi, J.P. and Bouchot, V. (2006) The Paleoproterozoic of Ghanaian Province: Geodynamic Model and Ore Controls, Including Regional Stress Modeling. *Precambrian Research*, **149**, 149-196. <https://doi.org/10.1016/j.precamres.2006.06.003>
- [10] Coulibaly, Y., Boiron, M.C., Cathelineau, M. and Kouamelan, A.N. (2008) Fluid

Immiscibility and Gold Deposition in the Birimian Quartz Veins of the Angovia deposit (Yaouré, Ivory Coast). *Journal of African Earth Sciences*, **50**, 234-254.
<https://doi.org/10.1016/j.jafrearsci.2007.09.014>

- [11] Soule-De-Lafont D. (1956) Le précambrien moyen supérieur de Bondoukou (Côte d'Ivoire). Bulletin du Service des mines (Dakar), Dakar, 163 p.
- [12] Lüdtke G. (1999) Géologie de la région Haute Comoé sud. Bulletin No.2, Direction de la Géologie, Abidjan, 164 p.
- [13] Toure S. (2007) Pétrologie et géochronologie du massif granitoïde de Bondoukou. Nord-Est de la Côte d'Ivoire. Évolution magmatique et contexte géodynamique au Protérozoïque inférieur. Relations avec le volcano-détritique du Zanzan, Koun, Tanda attribué au Tarkwaien du Ghana. Implications paléogéographiques. Université d'Abobo-Adjamé, Abidjan, 224 p.
- [14] Veh, S.A. (2016) Caractère petro-structurale du Tarkwaien et des formations associées de la région de Bondoukou (Nord-Est de la Côte d'Ivoire). Université Felix Houphouet Boigny, Abidjan, 56 p.
- [15] Aka, E.B.J.C. (2018) Etude géophysique par magnétométrie et polarisation provoquée des formations précambriniennes de la région de Gouméré (nord-est de la côte d'ivoire): caractérisation lithostructurale et implication à la connaissance de la minéralisation aurifère. Université Felix Houphouet Boigny, Abidjan, 191 p.
- [16] Milesi, J.P., Ledru, P., Feybesse, J.L., Dommange, A. and Marcoux, E. (1992) Early Proterozoic Ore Deposits and Tectonics of Birimian Orogenic Belt, West Africa. *Precambrian Research*, **58**, 305-344. [https://doi.org/10.1016/0301-9268\(92\)90123-6](https://doi.org/10.1016/0301-9268(92)90123-6)
- [17] Tagini, B. (1971) Esquisse structurale de la Côte d'Ivoire. Essai de géotectonique régionale. These de Doctorat, Faculte des sciences, Université de Lausanne, Lausanne, 266 p.
- [18] Kouamelan, A.N. (1996) Géochronologie et Géochimie des formations archéennes et protérozoïque de la dorsale de Man en Côte d'Ivoire. Implications pour la transition Archén protérozoïque. Université Rennes 1, Rennes, 284 p.
- [19] Pothin, K.B.K. and Gioan, P. (2000) Bilan géochronologique du socle précambrien de Côte d'Ivoire. *BIOTERRE, Revue internationale des sciences de la vie et de la terre*, **1**, 36-47.
- [20] Pitra, P., Kouamelan, A., Ballavre, M. and Peucat, J.-J. (2010) Palaeoproterozoic Highpressure Granulite Overprint of the Archean Continental Crust: Evidence for Homogeneous Crustal Thickening (Man Rise, Ivory Coast). *Journal of Metamorphic Geology*, **28**, 41-58. <https://doi.org/10.1111/j.1525-1314.2009.00852.x>
- [21] Koffi, G.R.-S., Kouamelan, A.N., Allialy, M.E., Coulibaly, Y. and Peucat, J.-J. (2020) Re-Evaluation of Leonian and Liberian Events in the Geodynamical Evolution of the Man-Leo Shield (West African Craton). *Precambrian Research*, **338**, Article ID: 105582. <https://doi.org/10.1016/j.precamres.2019.105582>
- [22] Kadio E. (1983) Aperçu sur le précambrien de Côte d'Ivoire: Géologie-métallogénie. *Journal of African Earth Sciences* (1983), **1**, 167-177.
[https://doi.org/10.1016/0899-5362\(83\)90009-X](https://doi.org/10.1016/0899-5362(83)90009-X)
- [23] Camil J. (1984) Pétrographie, chronologie des ensembles archéens et formations associées de la région de Man (Côte d'Ivoire) Implications pour l'histoire géologique du craton ouest-africain. l'Université d'Abidjan, Abidjan, 306 p.
- [24] Bonhomme, M. (1962) Contribution à l'étude géochronologique de la plate-forme de l'Ouest Africain. Annale des facultes des sciences. Universite Clermont-Ferrand, no. 1, 62 p.

- [25] Yacé I. (1993) Les complexes volcano-sédimentaires précambriens en Afrique de l'Ouest. *Symposium sur le protérozoïque inférieur*, Programme International de Correlation Géologique (PICG), Paris, No 234, 143 p.
- [26] Feybesse, J.L., Milesi, J.P., Johan, V., Dommangeat, A., Calvez, J.Y., Boher, M. and Abouchami, W. (1989) La limite Archéen-Protérozoïque inférieur de l'Afrique de l'Ouest: une zone de chevauchement majeur antérieure à l'accident de Sanssandra: l'exemple des régions d'Odienné et de Touba (Côte d'Ivoire). *Comptes Rendus de l'Académie des Sciences*, **309**, 1847-1853.
- [27] Tempier, P. (1986) Le Burkinién: Cycle orogénique majeur du protérozoïque inférieur en Afrique de l'Ouest. *Journée Scientifique du C.I.F.E.G*, **10**, 17-23.
- [28] Yacé, I. (2002) Initiation à la géologie. L'exemple de la Côte d'Ivoire et de l'Afrique de l'Ouest. Pétrologie, Géologie régionale. CEDA, SODEMI, Abidjan, 160 p.
- [29] Doumbia, S. (1997) Géochimie, géochronologie et géologie structurale des formations Birrimiennes de Katiola-Marabadiassa (Centre-Nord de la Côte d'Ivoire): Evolution magmatique et contexte géodynamique du Paléoprotérozoïque. Université d'Orléans, Orléans, 207 p.
- [30] Papon, A. (1973) Géologie et minéralisations du Sud-Ouest de la Côte d'Ivoire. Vol. 80, Mémoire du BRGM, Paris, 284 p.
- [31] Houssou, N.N., Kouadio, F.J.-L.H., Allaly, M.E., Kouassi, B.R. and Adingra, M.P.K. (2022) Geochemistry of Volcano-Sedimentary and Plutonic Formations of the Agbaou Gold Deposit, Ivory Coast. *Earth Science Research*, **11**, 76-97. <https://doi.org/10.5539/esr.v11n1p76>
- [32] Bonnault, D. and Sagatzky, J. (1950) Notice Explicative sur la feuille Bondoukou-Ouest. Carte géologique de reconnaissance à l'échelle 1/500000. Levés effectués de 1935 à 1937. Archives du Gouvernement Général de l'Afrique Occidentale Française, Dakar 25p.
- [33] Boya, T.K.L.-D., Kouadio, F.J.-L.H., Adingra, M.P.K., N'gatta, K.G.-L. and Kouamelan, A.N. (2022) Les métasédiments de Kouassi Bilékro, S/P de Kouassi Datékro, Est de la Côte d'Ivoire: Un exemple de pétrogénèse complexe au sein du bassin de la Comoé. *Afrique Science*, **20**, 57-71. <http://www.afriquescience.net>
- [34] Simeon, Y., Delor, C., Zeade, Z., Kone, Y., Yao, B., Vidal, M., Diaby, I., Konan, G., Dje, B.I., N'da, D., Dommangeat, A., Cautru, J.P., Guerrot, C. and Chiron, J.-C. (1995) Notice explicative de la carte géologique de la Côte d'Ivoire à 1/200000, feuille Agnibilékro. Mémoire de la Direction des Mines et de la Géologie de la Côte d'Ivoire, Abidjan, 5-8, 13.
- [35] Janousek, V., Farrow, C.M. and Erban, V. (2006) Interpretation of Whole-Rock Geo-Chemical Data in Igneous Geochemistry: Introducing Geochemical Data Toolkit (GCDkit). *Journal of Petrology*, **47**, 1255-1259. <https://doi.org/10.1093/petrology/egl013>
- [36] Middlemost, E.A.K. (1994) Naming Materials in the Magma/Igneous Rock System. *Earth Science Reviews*, **37**, 215-224. [https://doi.org/10.1016/0016-8252\(94\)90029-9](https://doi.org/10.1016/0016-8252(94)90029-9)
- [37] Irvine, T.N. and Baragar, W.R.A. (1971) A Guide to the Chemical Classification of the Common Volcanic Rocks. *Canadian Journal of Earth Sciences*, **8**, 523-548. <https://doi.org/10.1139/e71-055>
- [38] Pearce, J.A. and Cann, J.R. (1973) Tectonic Setting of Basic Volcanic Rocks Determined Using Trace Element Analyses. *Earth and Planetary Science Letters*, **19**, 290-300. [https://doi.org/10.1016/0012-821X\(73\)90129-5](https://doi.org/10.1016/0012-821X(73)90129-5)
- [39] Werner, C.D. (1987) Saxonian Granulites: A Contribution to the Geochemical Di-

- agnosis of Original Rocks in High-Metamorphic Complexes. *ZfS-Mitteilungen*, **133**, 221-250.
- [40] Herron, M.M. (1988) Geochemical Classification of Terrigenous Sands and Shales from Core or Log Data. *Journal of Sedimentary Petrology*, **58**, 820-829. <https://doi.org/10.1306/212F8E77-2B24-11D7-8648000102C1865D>
- [41] Pearce, J.A., Harris, N.B.W. and Tindle, A.G. (1984) Trace Element Discrimination Diagrams for the Tectonic Interpretation of Granitic Rocks. *Journal of Petrology*, **25**, 956-983. <https://doi.org/10.1093/petrology/25.4.956>
- [42] Pearce, J.A. (1983) Role of the Sub-Continental Lithosphere in Magma Genesis at Active Continental Margins. In: Hawkesworth, C.J. and Norry, M.J., Eds., *Continental Basalts and Mantle Xenoliths*, Shiva Publishing, Nantwich, 230-249.
- [43] Pearce, J.A. and Peate, D.W. (1995) Tectonic Implications of the Composition of Volcanic Arc Magmas. *Annual Review of Earth and Planetary Sciences*, **23**, 251-285. <https://doi.org/10.1146/annurev.ea.23.050195.001343>
- [44] Wood, D.A. (1980) The Application of a Th-Hf-Ta Diagram to Problems of Tectonomagmatic Classification and to Establishing the Nature of crustal Contamination of Basaltic Lavas of the British Tertiary Volcanic Province. *Earth and Planetary Science Letters*, **50**, 11-30. [https://doi.org/10.1016/0012-821X\(80\)90116-8](https://doi.org/10.1016/0012-821X(80)90116-8)
- [45] Roser, B.P. and Korsch, R.J. (1986) Determination of Tectonic Setting of Sandstone-Mudstone Suites Using SiO₂ Content and K₂O/Na₂O Ratio. *The Journal of Geology*, **94**, 635-650. <https://doi.org/10.1086/629071>
- [46] Perrouyt, S. (2012) Evolution structurale de la ceinture minéralisée d'Ashanti, SO du Ghana. Université de Toulouse, Toulouse, 233 p.
- [47] Baratoux, L., Metelka, V., Naba, S., Jessell, M.W., Gregoire, M. and Ganne, J. (2011) Juvenile Paleoproterozoic Crust Evolution during the Eburnean Orogeny (~2.2-2.0 Ga), Western Burkina Faso. *Precambrian Research*, **191**, 18-45. <https://doi.org/10.1016/j.precamres.2011.08.010>
- [48] Bossiere, G., Bonkoungou, I., Peucat, J.-J. and Pupin, J.-P. (1996) Origin and Age of Paleoproterozoic Conglomerates and Sandstones of the Tarkwaian Group in Burkina Faso, West Africa. *Precambrian Research*, **80**, 153-172. [https://doi.org/10.1016/S0301-9268\(96\)00014-9](https://doi.org/10.1016/S0301-9268(96)00014-9)
- [49] Pouplet, A., Vidal, M., Delor, C., Simeo, Y. and Alric, G. (1996) Le volcanisme birimien du nord-est de la Côte d'Ivoire, mise en évidence de deux phases volcanotectoniques distinctes dans l'évolution géodynamique du Paléoprotérozoïque. *Bulletin de la Société Géologique de France*, **167**, 529-541.
- [50] Vidal, M., Delor, C., Pouplet, A., Simeon, Y. and Alric, G. (1996) Evolution géodynamique de l'Afrique de l'Ouest entre 2,2 et 2 Ga: Le style archéen des ceintures vertes et des ensembles sédimentaires birimiens du nord-est de la Côte d'Ivoire. *Bulletin de la Société Géologique de France*, **167**, 307-319.
- [51] Houssou, N.N. (2013) Etude pétrologique, structurale et métallogénique du gisement aurifère d'Aghabou, Divo, Côte d'Ivoire. Université Félix Houphouët-Boigny, Abidjan, 177 p.
- [52] Ouattara, Z. (2015) Caractères lithostratigraphiques, structural, géochimique et métallogénique du gisement d'or de Bonikro, sillon birimien de Fettékro, Centre-Sud de la Côte d'Ivoire. Université Félix Houphouët-Boigny, Abidjan, 275 p.
- [53] Coulibaly, I. (2018) Pétrographie des volcanites et platonites de la partie Sud du sillon volcanosédimentaire de Toumodi-Fétékro. Université Félix Houphouët-Boigny, Abidjan, 221p.

- [54] Mortimer, J. (1992) Lithostratigraphy of the Early Proterozoic Toumodi Volcanic Group in Central Côte d'Ivoire: Implications for Birrimian Stratigraphic Models. *Journal of African Earth Sciences (and the Middle East)*, **14**, 81-91. [https://doi.org/10.1016/0899-5362\(92\)90057-J](https://doi.org/10.1016/0899-5362(92)90057-J)
- [55] Leake, M.H. (1992) The Petrogenesis and Structural History of the Northern Sector of the Fettekro Greenstone Belt, Dabakala Region, NE Côte d'Ivoire. University of Portsmouth, Portsmouth, 315 p.
- [56] Lompo, M. (2009) Geodynamic Evolution of the 2.25-2.0 Ga Paleoproterozoic magmatic Rocks in the Man-Leo Shield of the West African Craton. A Model of Subsidence of an Oceanic Plateau. In: Reddy, S.M., Mazumder, R., Evans, D.A.D. and Collins, A.S., Eds., *Palaeoproterozoic Supercontinents and Global Evolution*, Vol. 323, Geological Society of London, London, 231-254. <https://doi.org/10.1144/SP323.11>
- [57] Fitton, J.G., James, D., Kempton, P.D., Ormerod, D.S. and Leenam, W.P. (1988) The Role of the Lithospheric Mantle in the Generation of the Late Cenozoic Basic Magmas in the Western United States. *Journal of Petrology, Special Lithosphere*, 331-349. https://doi.org/10.1093/petrology/Special_Volume.1.331
- [58] Dampare, S.B., Shibata, T., Asiedu, D.K., Osae, S. and Banoeng-Yakubo, B. (2008) Geochemistry of Paleoproterozoic Metavolcanic Rocks from the Southern Ashanti Volcanic Belt, Ghana: Petrogenetic and Tectonic Setting Implications. *Precambrian Research*, **162**, 403-423. <https://doi.org/10.1016/j.precamres.2007.10.001>
- [59] Lesher, C.M., Goodwin, A.M., Campbell, I.H. and Gorton, M.P. (1986) Trace Element Geochemistry of Ore-Associated and Barren, Felsic Metavolcanic Rocks in the Superior Province. *Canada Journal of Earth Sciences*, **23**, 222-237. <https://doi.org/10.1139/e86-025>
- [60] Hart, S., Coetzee, M., Workman, R., Blusztajn, J., Johnson, K., Sinton, J., Steinberger, B. and Hawkins, J. (2004) Genesis of the Western Samoa Seamount Province: Age, Geochemical Fingerprint and Tectonics. *Earth and Planetary Science Letters*, **227**, 37-56. <https://doi.org/10.1016/j.epsl.2004.08.005>